Impact of Star Connection Layouts on the Control of Multiphase Induction Motor Drives Under Open-Phase Fault

Giacomo Sala, *Member, IEEE*, Michele Mengoni, *Member, IEEE*, Gabriele Rizzoli, Michele Degano, *Member, IEEE*, Luca Zarri, *Senior Member, IEEE*, and Angelo Tani

***Abstract*—This article presents a postfault control algorithm that minimizes the stator Joule losses in multiphase induction machines under an open-phase fault and for different star connection layouts. The key novelty is that the algorithm can be applied to any configuration of a multi-*n*-phase machine, independently of the connection of the neutral points. The latter is analytically derived and is based on the space vector representation of the machine model. In addition, it is shown that a low number of neutral points helps to reduce the winding losses in case of an open-phase fault but requires additional control regulators and computational efforts. The theory is applied to an asymmetrical quadruple-three-phase induction machine, which is configured to represent five different motor layouts. Finally, experimental results are presented to validate the control algorithm. The optimal solution that is given in this article can be employed for the control of symmetrical or asymmetrical multiphase machines with different star connection layouts and in any open-phase postfault operation.**

***Index Terms*—Circuit faults, induction motors, multiphase machines, postfault control (PFC), power system reliability, variable-speed drives.**

I. Introduction

WHEN reliability is an essential feature, a standard approach to enhance the fault tolerance is the redundancy of the critical systems. In the field of electric drives, the use of multiphase machines is considered as one of the most promising fault-tolerant technologies [1], [2]. An initial classification of multiphase drives can be done considering the layout of the stator phases. Therefore, multiphase drives are commonly distinguished in multiphase, multisingle-phase, and multithree-phase ones [3].

Manuscript received May 14, 2020; revised August 13, 2020; accepted September 8, 2020. Date of publication September 15, 2020; date of current version November 20, 2020. Recommended for publication by Associate Editor A. Muetze. *(Corresponding author: Giacomo Sala.)*

Giacomo Sala, Michele Mengoni, Gabriele Rizzoli, Luca Zarri, and Angelo Tani are with the Department of Electrical and Electronic Engineering, University of Bologna, 40126 Bologna, Italy (e-mail: giacomo.sala5@unibo.it; michele.mengoni@unibo.it; gabriele.rizzoli@unibo.it; luca.zarri@mail.ing.unibo.it; angelo.tani@unibo.it).

Michele Degano is with the Power Electronics, Machines and Control Group, Department of Electrical and Electronic Engineering, The University of Nottingham, Nottingham NG7 2RD, U.K., and also with the Key Laboratory of More Electric Aircraft Technology of Zhejiang Province, Power Electronics, Machines and Control Group, University of Nottingham Ningbo Campus, Ningbo 315100, China (e-mail: michele.degano@nottingham.ac.uk).

Color versions of one or more of the figures in this article are available online at https://ieeexplore.ieee.org.

Digital Object Identifier 10.1109/TPEL.2020.3024205

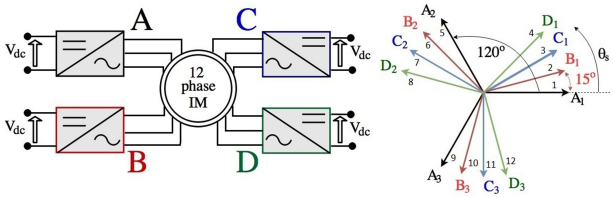

Fig. 1. Conceptual scheme of the analyzed drive in its quadruple-three-phase layout (left) and magnetic axes of the 12-phase induction machine (right). The axes of each three-phase subsystem are equally colored and are shifted by 15° with respect to each other.

In a multiphase drive where a single converter feeds all the phases connected to a single neutral point, a variety of critical faults may affect the system and lead to the complete failure of the drive (dc-bus failure, power converter fault, short circuits in the winding, etc.). To avoid the failure of the system in these scenarios, one of the most reliable layouts is the multisingle-phase, where independent converters feed galvanically separated phases. However, this solution may be complicated, expensive, and with reduced efficiency [4]. The multithree-phase layout is an intermediate solution, where each three-phase winding is star connected and can be fed by an independent inverter. Multi-*n*-phase layouts can also be adopted, but the three-phase one is favorite because of the maturity of the related power electronics technology. For example, Fig. 1 illustrates the multithree-phase layout of the 12-phase machine considered for the validation of the algorithm proposed in this article.

Multiphase drives are redundant by definition: when a phase is open, the other ones can compensate for the missing power and reduce the performance derating. However, the optimal postfault strategy is challenging to generalize, because it depends on the machine topology and the control algorithm.

Some research lines dealt with methodologies for the definition of optimum current references to obtain a better torque response. These methods have been developed for machines with different layouts and numbers of phases by using genetic algorithms [5] and numerical computations based on analytical formulations [6] and categorizing the angles between the adjacent healthy phases [7]. The fault-tolerant control systems have also been integrated with diagnostic algorithms that take into account the converter layout [8]. In addition, as confirmed by recent studies, the performance of conventional control schemes for

multiphase drives significantly deteriorates under open-phase faults and requires a change of the architecture toward a fault-tolerant scheme [9]. This phenomenon is well described also in [10], where a self-healing control scheme is proposed. In that article, the architecture of the control scheme does not change when a fault happens, and no fault detection is required, thanks to an extended phase locked loop (EPLL). The EPLL is embedded with an automatic adjustment of the reference currents in the harmonic subspace limited by a minimum loss coefficient.

This article investigates how the star connection layout affects the performance of multi-n-phase induction machines under open-phase fault conditions. Some postfault algorithms have already been proposed for induction machines with a single star and an odd number of phases [11]. Later, they have been extended to dual-three-phase machines with single or double isolated neutral points [12], [13]. Various fault-tolerant algorithms have been compared, showing how to obtain the maximum output torque under open-phase fault scenarios. However, at the current state of the art, several postfault algorithms require the numerical solution of an optimization problem with convergence methods that avoid local maximums and guarantee a global optimum solution [14]. These methods can be applied to any electrical machine. They have also been extended to delta-connected layouts [15]–[17] and to customized inverters or peculiar winding layouts, e.g., to enhance the performance or the fault-tolerant capabilities [18], [19]. If the postfault control (PFC) aims to minimize the stator copper losses, it is also possible to find the optimal analytical solution in closed form, as demonstrated for particular configurations of the windings [11], [20], [21] and converter architectures [22], [23].

One of the aims of the current research is to develop fault-tolerant algorithms that are as general as possible. Furthermore, the analysis of the stator Joule losses and their distribution in the machine winding has a significant impact on the postfault thermal stress [24]–[27], making its minimization a priority for postfault algorithms of electrical machines.

With reference to these topics, the main contributions of this article are listed hereafter.

1) The article defines a generalized method for PFC of multiphase machines in case of open-phase faults, which can be analytically derived and easily adapted to different machine layouts. For the sake of generality, the stator phases are arranged into a set of n-phase windings, where the neutral points of each winding can be connected to or insulated from the neutral points of the other windings, depending on the machine layout. To the best of the authors' knowledge, such a method is not available in the literature.
2) In case of an open-phase fault, it is necessary to find the optimal set points of the machine currents to mitigate the effect of the fault. It turns out that the system of equations that solves this problem depends on the specific machine layout and, in some cases, is even undetermined. To overcome this difficulty, the developed algorithm minimizes the Joule losses and finds an explicit solution by using the pseudoinverse operator and the vector space decomposition (VSD) approach [28].

Finally, experimental results are presented to validate the PFC and to provide an in-depth comparison of the developed techniques for the single-, double-, and quadruple-star layouts of a 12-phase machine.

II. Machine Equations in Healthy and Faulty Conditions

The machine model is developed decomposing the machine variables in multiple vector subspaces or planes. Consequently, the equations written in terms of space vectors (SVs) can be used to evaluate the electromechanical behavior of the machine and develop a suitable control algorithm.

A. SV Representation

VSD is widely used for the analysis of multiphase machines and allows representing any set of electrical quantities $y_1, y_2, \ldots, y_m$ in terms of their respective SVs $\bar{y}_1, \bar{y}_2, \ldots, \bar{y}_m$ defined as follows:

$$\bar{y}_\rho = \frac{2}{m} \sum_{k=1,2,\ldots}^{m} y_k e^{j\rho\varphi_k} \tag{1}$$

where φ_k is the angular position of the magnetic axis of the kth phase. In a multi-n-phase machine with m/n n-phase subwindings arranged symmetrically, the angle φ_k can be calculated as follows:

$$\varphi_k = \text{mod}\left(k-1, \frac{m}{n}\right)\Delta\varphi + \left\lfloor (k-1)/\left(\frac{m}{n}\right)\right\rfloor \frac{2\pi}{n} \tag{2}$$

where mod is the modulo operation that finds the remainder after $(k-1)$ is divided by $\frac{m}{n}$, $\lfloor\rfloor$ is the floor operation that rounds its argument down to an integer, and $\Delta\varphi$ is the angular shift among neighboring subwindings. In addition, the first phase ($k=1$) is assumed aligned with the stator reference frame ($\varphi_1 = 0$).

In case of distributed windings with m phases, the angular shift $\Delta\varphi$ of the subwindings is $\frac{2\pi}{m}$ for a symmetrical layout and $\frac{\pi}{m}$ for an asymmetrical layout (as illustrated in Fig. 1).

If the machine features an odd number of phases, the inverse transformation of (1) can be simplified as follows:

$$y_k = \frac{\bar{y}_m}{2} e^{-jm\varphi_k} + \sum_{\rho=1,3,5,\ldots}^{m-2} \Re\{\bar{y}_\rho e^{-j\rho\varphi_k}\} \tag{3}$$

where $\Re$ is the real operator.

Conversely, for a machine with an even number of phases, the inverse transformation of (1) becomes

$$y_k = \sum_{\rho=1,3,5\ldots}^{m-1} \Re\{\bar{y}_\rho e^{-j\rho\varphi_k}\}. \tag{4}$$

Equations (1)–(4) can be used to develop models and control algorithms for multiphase machines, independently of their star connection layouts.

B. Model of a Multiphase Induction Machine

The stator and rotor equations describing a multiphase induction machine are written in the stator and rotor reference frames,

respectively, in terms of SVs as follows:

$$\bar{v}_{S,\rho} = R_S \bar{i}_{S,\rho} + \frac{d\bar{\phi}_{S,\rho}}{dt} \tag{5}$$

$$0 = R_{R,\rho} \bar{i}_{R,\rho} + \frac{d\bar{\phi}_{R,\rho}}{dt} \tag{6}$$

where R_S and $R_{R,\rho}$ are the stator phase resistance and equivalent rotor resistance in the ρth subspace, respectively. Neglecting the iron saturation, the slotting effect, and the high-order field harmonics with $\rho > 1$, the stator and rotor flux vectors are as follows:

$$\bar{\phi}_{S,1} = L_{S,1} \bar{i}_{S,1} + M_1 \bar{i}_{R,1} e^{j\theta_m} \tag{7}$$

$$\bar{\phi}_{R,1} = L_{R,1} \bar{i}_{R,1} + M_1 \bar{i}_{S,1} e^{-j\theta_m} \tag{8}$$

$$\bar{\phi}_{S,\rho} = l_{S,\rho} \bar{i}_{S,\rho}, \quad \rho = 3, 5, \ldots \tag{9}$$

$$\bar{\phi}_{R,\rho} = l_{R,\rho} \bar{i}_{R,\rho}, \quad \rho = 3, 5, \ldots \tag{10}$$

where θ_m is the angular displacement between the stator and rotor reference frames in electrical radians, $L_{S,1}$, $L_{R,1}$, and M_1 are the stator, rotor, and mutual inductances of the fundamental harmonic, respectively while $l_{S,\rho}$ and $l_{R,\rho}$ are, respectively, the equivalent stator and rotor leakage inductances in the ρth subspace. Finally, under the assumption that the high-order spatial components of the magnetic field are negligible, the electromagnetic torque can be written as follows:

$$T = \frac{m}{2} p M_1 \Re\{j \bar{i}_{R,1} e^{j\theta_m} \bar{i}^*_{S,1}\} \tag{11}$$

where * is used to indicate the conjugate operator ($j^* = -j$), and p is the number of pole pairs. Equations (5)–(11), together with the equation of motion, can be used to evaluate the electromechanical behavior of the machine.

C. Model of a 12-Phase Induction Machine

Replacing (7)–(10) in (5) and (6) leads to the following equations, which are valid for a 12-phase induction machine:

$$\bar{v}_{S,1} = R_S \bar{i}_{S,1} + L_{S,1} \frac{d\bar{i}_{S,1}}{dt} + M_1 \frac{d(\bar{i}_{R,1} e^{j\theta_m})}{dt} \tag{12}$$

$$0 = R_{R,1} \bar{i}_{R,1} + L_{R,1} \frac{d\bar{i}_{R,1}}{dt} + M_1 \frac{d(\bar{i}_{S,1} e^{-j\theta_m})}{dt} \tag{13}$$

$$\bar{v}_{S,\rho} = R_S \bar{i}_{S,\rho} + l_S \frac{d\bar{i}_{S,\rho}}{dt}, \quad \rho = 3, 5, 7, 9, 11. \tag{14}$$

Equations (12)–(14) can be used to analyze the behavior of the different layouts of a 12-phase machine ($m = 12$). The stator windings can be connected to each other in different ways, depending on the number of insulated neutral points. For example, the possible connections of four three-phase windings are shown in Fig. 2. On the one hand, the single-star layout presents more degrees of freedom in the current control and is of interest for the implementation of control systems based on high-order field harmonics or diagnostic algorithms that employ the same harmonics to obtain information on the parameters and the behavior of the electrical machine. This layout is also the one that allows the best postfault performance of the drive. On the other hand, the multi-three-phase solution features galvanic insulation of the subwindings. This insulation allows supplying each subwinding with an independent inverter connected to a separated dc link, resulting in a modular converter architecture that is suitable for the implementation of power-sharing control schemes and the employment of conventional three-phase inverter technologies. Intermediate solutions (as the double-six-phase layouts in Fig. 2) represent possible alternatives to mediate between the two aforementioned opposite architectures.

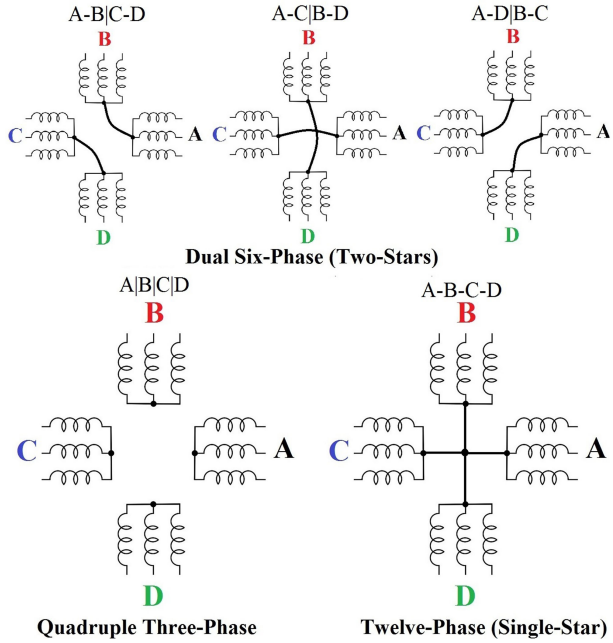

Fig. 2. Most interesting star connection layouts of a 12-phase distributed-winding machine.

D. Constraints Due to Star Connections

In a machine with m phases and N_{st} insulated neutral points (or stars), the degrees of freedom in the control of the phase currents are $m - N_{\text{st}}$. The phases of the hth star-connected winding are those whose indexes belong to the set W_h. Owing to the star connections, the sum of the currents flowing toward the same neutral point is zero, i.e.,

$$\sum_{k \in W_h} i_k = 0, \quad h = 1, 2, \ldots, N_{\text{st}}. \tag{15}$$

By introducing the inverse transformation (3) or (4), it is possible to express the constraints described by (15) in terms of current SVs. It turns out that only some current SVs are constrained by (15), whereas the fundamental current SV $\bar{i}_1$ is not affected, because it vanishes from the equation. As a result, it is possible to rewrite (15) in terms of SV components by using the following matrix notation:

$$C \mathbf{i}_{\text{aux}} = 0 \tag{16}$$

where C is a full-rank N_{st}-by-$(m-2)$ matrix, and $\mathbf{i}_{\text{aux}}$ is the column vector of the $\alpha\beta$ components of the current SVs different from $\bar{i}_1$. The expression of $\mathbf{i}_{\text{aux}}$, respectively, for systems with

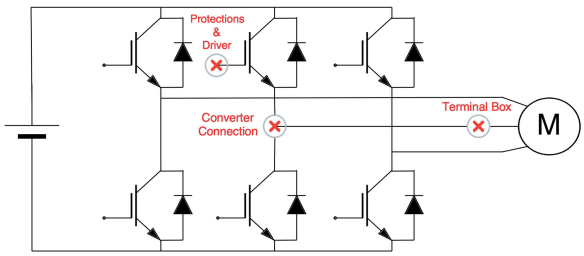

Fig. 3. Open-phase fault typologies.

odd and even numbers of phases, is as follows:

$$\mathbf{i}_{\text{aux}} = [i_{3\alpha}\ i_{3\beta}\ i_{5\alpha}\ i_{5\beta}\ \ldots\ldots\ i_{m\alpha(\beta)}]^{\top} \tag{17}$$

$$\mathbf{i}_{\text{aux}} = [i_{3\alpha}\ i_{3\beta}\ i_{5\alpha}\ i_{5\beta}\ \ldots\ldots\ i_{(m-1)\alpha}\ i_{(m-1)\beta}]^{\top} \tag{18}$$

where the operator " $\top$ " identifies the transpose operator.

The SVs $\bar{i}_{\rho}$ with $\rho > 1$ are called auxiliary vectors to distinguish them from the fundamental one $\bar{i}_1$, which can be rewritten as a column vector as follows:

$$\mathbf{i}_1 = [i_{1\alpha}\ i_{1\beta}]^{\top}. \tag{19}$$

Equation (16) is used in Section III, together with the constraints resulting from an open-phase fault, in order to define an optimized postfault algorithm.

E. Model of a Multiphase Stator Winding in Case of Open-Phase Fault

The zeroing of a stator current may be caused by a fault in the converter or the machine, as shown in Fig. 3 for a standard three-phase drive. The breakdown of the switching devices or the activation of the active and passive protections of the drive (e.g., the desaturation protection, that turns the switches OFF in order to avoid dangerous overcurrents) can easily cause the uncontrolled phase currents to be zero. Also, this happens in case of actual open-phase faults due to the disconnection of the phases from the terminal box, the neutral point, or the terminals of the inverter. This might result from assembly mistakes or the deterioration of the connections.

In the postfault condition, the machine operates under the constraints that the currents of the faulty phases $k_1, k_2, \ldots k_{N_f}$ are zero, i.e.,

$$i_{k_f} = 0, \qquad f = 1, 2, \ldots, N_f. \tag{20}$$

In terms of current SVs, (20) can be rewritten using the inverse Clarke's transformation (3) or (4) and expressed in matrix form as follows:

$$B\mathbf{i}_1 + A\mathbf{i}_{\text{aux}} = 0 \tag{21}$$

where B is an N_f-by-2 matrix, and A is an N_f-by-$(m-2)$ matrix, respectively, defined as follows:

$$B = \begin{bmatrix} c_{1,k_1} & \cdots & \cdots & c_{1,k_{N_f}} \\ s_{1,k_1} & \cdots & \cdots & s_{1,k_{N_f}} \end{bmatrix}^{\top} \tag{22}$$

$$A = \begin{bmatrix} c_{3,k_1} & \cdots & \cdots & c_{3,k_{N_f}} \\ s_{3,k_1} & \cdots & \cdots & s_{3,k_{N_f}} \\ c_{5,k_1} & \cdots & \cdots & c_{5,k_{N_f}} \\ s_{5,k_1} & \cdots & \cdots & s_{5,k_{N_f}} \\ \cdots & \cdots & \cdots & \cdots \\ \cdots & \cdots & \cdots & \cdots \\ c_{(m-1)_{\text{odd}},k_1} & \cdots & \cdots & c_{(m-1)_{\text{odd}},k_{N_f}} \\ s_{(m-1)_{\text{odd}},k_1} & \cdots & \cdots & s_{(m-1)_{\text{odd}},k_{N_f}} \\ c_{(m)_{\text{odd}},k_1} & \cdots & \cdots & c_{(m)_{\text{odd}},k_{N_f}} \end{bmatrix}^{\top} \tag{23}$$

where $c_{\rho,k_f} = \cos(\rho\varphi_{k_f})$, $s_{\rho,k_f} = \sin(\rho\varphi_{k_f})$, and φ_{k_f} is the electrical angle of the faulty phase with index k_f, as defined in (2).

In the next section, the postfault constraint (21) is combined with the one resulting from the presence of insulated neutral points (16) in order to find the analytical solution for the optimized postfault algorithm.

III. Postfault Control Algorithm With Minimum Copper Joule Losses

Managing an open-phase fault is essential to ensure the operation of the drive (e.g., to avoid instability phenomena or unexpected extra losses) and to optimize its postfault performance. Furthermore, such a control scheme could be used to keep the current of one or more phases at zero in case of necessity, although a fault has not occurred yet. The advantages of zeroing the currents in particular phases are twofold: reduce the related copper losses and minimize the stress of the emergency ac breakers for the disconnection of these phases. For example, if a fault or a localized temperature increase is detected, the current of the phase placed next to that area can be controlled to zero in order to avoid the accelerated aging of the insulation. Furthermore, in case of a redundant converter architecture (as in a multi-three-phase configuration), it would be possible to control to zero the power of one subconverter, so that its dc link could be opened with a limited effort and without incurring in the phenomenon of electric arc. Then, the converter could be replaced or its maintenance could be carried out without unscheduled service interruption. Because of the importance of the open-phase fault-tolerant algorithm in highly reliable drives, this section shows a general approach to define an optimized postfault algorithm for a multiphase machine analytically. The fundamental contributions to the electromagnetic torque and flux depend on $\bar{i}_1$, which can be assumed as a known quantity calculated by the control system depending on the operating conditions. Therefore, the PFC problem consists in finding a solution for $\mathbf{i}_{\text{aux}}$ that satisfies (16) and (21). The system of equations obtained combining (16) and (21) has $N_{\text{st}} + N_f$ rows and $m-2$ unknown variables, so it is usually underdetermined being $N_{\text{st}} + N_f < m-2$. Among the possible solutions of (16) and (21), the one that minimizes the total stator copper losses can be found analytically.

The stator copper losses are as follows:

$$P_J = \sum_{k=1}^{m} R_s i_k^2 = \frac{m}{2} R_s \mathbf{i}_1^\top \mathbf{i}_1 + \frac{m}{2} R_s \mathbf{i}_{\text{aux}}^\top \mathbf{i}_{\text{aux}}. \tag{24}$$

The solution to the problem of minimizing (24) with the constraints (16) and (21) can be written in closed form, as explained hereafter.

Let D be the $(N_{\text{st}} + N_f)$-by-$(m-2)$ matrix obtained by appending the rows of C to the rows of A

$$D = \begin{bmatrix} A \\ C \end{bmatrix} \tag{25}$$

and let E be the $(N_{\text{st}} + N_f)$-by-2 matrix obtained by appending N_{st} null rows to the rows of B.

$$E = \begin{bmatrix} B \\ 0_{(N_{\text{st}},2)} \end{bmatrix}. \tag{26}$$

The rank of D is $(N_{\text{st}} + N_f)$. Equations (16) and (21) can be written in compact form as follows:

$$D\mathbf{i}_{\text{aux}} + E\mathbf{i}_1 = 0. \tag{27}$$

The solution to the optimization problem is

$$\mathbf{i}_{\text{aux}} = F\mathbf{i}_1 \tag{28}$$

where F is an $(m-2)$-by-2 matrix defined as follows:

$$F = -D^+ E. \tag{29}$$

The operator "+" applied to D in (29) represents the Moore–Penrose inverse of D, more precisely its right pseudoinverse matrix defined as follows:

$$D^+ = D^\top (DD^\top)^{-1}. \tag{30}$$

The resulting matrix F represents a unique set of constants, which relates the auxiliary SVs $\mathbf{i}_{\text{aux}}$ to $\mathbf{i}_1$ for each fault configuration and layout of the neutral points and minimizes the stator copper losses. The values of F are not affected by the operating condition of the machine and need to be calculated only once, when the fault is detected. In addition, these values can be calculated offline and stored on a conventional control platform such as a DSP. As an example, the aspect of matrices A, B, C, and F is analyzed in the Appendix and presented in Table III for a particular fault scenario.

In a machine without star connections, i.e., a multi-single-phase or an open-end winding layout, the matrix F in (28) and (29) can be simplified as follows:

$$F = -A^\top [AA^\top]^{-1} B. \tag{31}$$

When the machine has an odd number of symmetrically distributed phases and a single star, C is a single-row matrix. The entry in the $(m-2)$th column is 1, while the other entries are zero. In other terms, it is enough to neglect the one-dimensional current SV component related to the zero-sequence current in the A matrix (i.e., the mth column of A). In this case, in agreement with the relationship found in [11], (31) can still be used. In conclusion, (28) can be employed to directly find the optimal solution for symmetrical or asymmetrical multiphase windings with different layouts of the star connections and in any open-phase postfault operation.

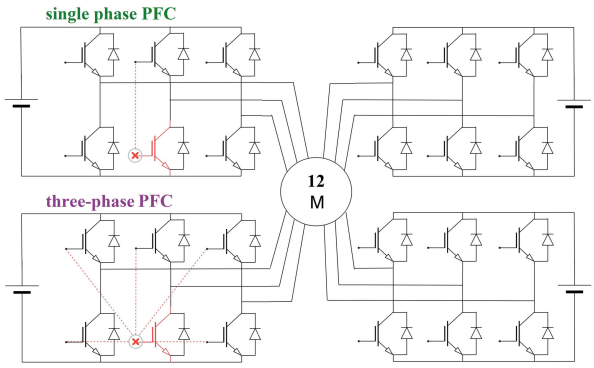

Fig. 4. Open-phase fault management in a quadruple-three-phase converter: "single-phase PFC" logic (left top) and "three-phase PFC" logic (left bottom).

IV. Simplified Postfault Control Algorithm for Multi-n-Phase Drives

This section briefly summarizes a simplified control algorithm suitable for multi-n-phase windings. The algorithm is based on an analytical approach and is suitable for drives with a high number of phases and star connections (e.g., a quadruple-three-phase one), where the application admits a high reduction in the machine performance in the postfault operation.

The problem of PFC is linked to the concept of power sharing. According to this technique, the overall power of a multi-n-phase drive can be unequally split among a set of independent n-phase converters [24], [29]–[31]. A particular case of power sharing is when the output power (or current) of a converter is zero. This case perfectly matches the PFC of the machine.

Different PFC strategies can be defined, as shown in Fig. 4, for a quadruple-three-phase electric drive. After the failure of one device, two strategies seem more reasonable. The first one consists of disabling the switches of the faulty phase ("single-phase PFC"), and the second one consists of disabling all the switches of the inverter involved in the fault ("three-phase PFC"). When commercial three-phase inverters are used, the latter approach is simpler. The three-phase PFC strategy can also be preferred because it avoids the low-frequency distortion of the power flows at the dc links of the converter in case the converter is built of independent modules connected to insulated dc links.

The next section shows the proposed control architectures of a 12-phase induction motor drive for various winding layouts and compares them in terms of control design and performance.

V. Control Architecture

A standard three-phase machine is controlled through the fundamental SV $\bar{i}_{S,1}$. To control this current vector, two proportional–integral (PI) regulators are usually employed. In general, the minimum number of PI regulators required to control the current SVs of an m-phase machine with N_{st} stars is

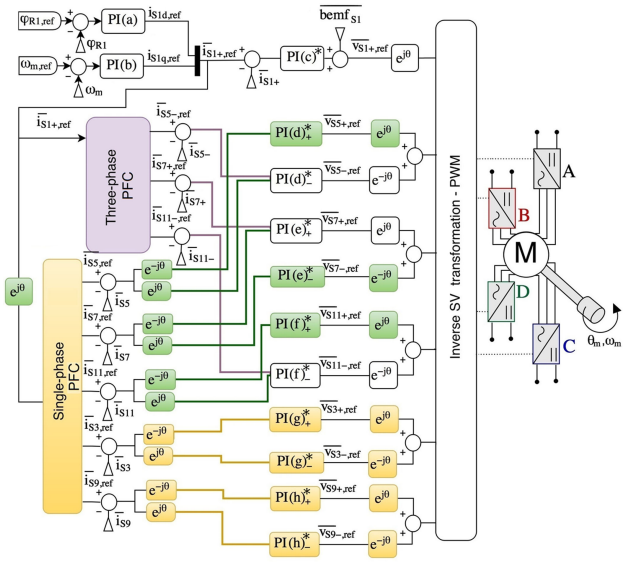

Fig. 5. Control algorithm of a 12-phase machine in different conditions: healthy or "three-phase PFC" with four insulated neutral points (white), faulty with four independent stars and "single-phase PFC" (white and green), healthy with double-six-phase or single star (white and yellow), and faulty with double-six-phase or single star and "single-phase PFC" (white, green, and yellow).

equal to the number of independently controllable currents, i.e., $m - N_{\text{st}}$.

For example, Fig. 5 shows the control scheme of a quadruple-three-phase machine ($m = 12$ and $N_{\text{st}} = 4$). The signals at the input of the PI controllers are complex quantities, so each block highlighted with a "*" in Fig. 5 must be intended as a couple of PI regulators, respectively, for the d and q components of the signals. The eight PI current controllers colored in white are the ones required to control the healthy machine ($m - N_{\text{st}} = 8$). Two current PI controllers are required to track the reference set points of the fundamental space, whereas the other six PI controllers are used to keep at zero the currents in the harmonic subspaces.

Conversely, if all the subwindings were connected together to the same neutral point ($m = 12$ and $N_{\text{st}} = 1$, i.e., $m - N_{\text{st}} = 11$), the number of PI regulators needed to control the machine would increase to $m - 1$, i.e., 11.

However, a postfault algorithm requires, in general, more PI regulators than the normal control system. In fact, the trajectories of some current SVs are often elliptic (even degenerate) rather than circular. For each SV with an elliptic trajectory, it is necessary to use a pair of PI regulators, implemented in counter-rotating reference frames, in order to ensure a theoretical zero error at the steady state. Hence, the PI regulators for the control of these SVs double. Although, for each faulty phase, the number of the degrees of freedom decreases by one, it results that the number of PI regulators for the control scheme of the faulty machine needs to be increased to obtain an effective tracking of the current references.

It is possible to analyze how the control architecture changes depending on the layout of the winding, the type of fault, and the adopted postfault strategy. Under the assumption of an

TABLE I
MAIN MACHINE PARAMETERS (50 Hz)

Symbol	Quantity	Value
P_{rated}	rated power	$10\,kW$
T_{rated}	rated torque	$16\,Nm$
$\lvert\bar{i}_{S,1,rated}\rvert$	main current vector magnitude	$16\,A_{pk}$
$i_{S,1,d,rated}$	rated d-axis current	$10\,A_{pk}$
I_{max}	maximum phase current	$23\,A_{pk}$
$\lvert\bar{v}_{S,1,rated}\rvert$	rated phase voltage	$186\,V_{pk}$
R_S	stator resistance	$0.188\,\Omega$
$R_{R,1}$	rotor resistance for the subspace 1	$0.156\,\Omega$
$L_{S,1}, L_{R,1}$	stator and rotor inductances	$12.8\,mH$
M_1	mutual inductance	$12.0\,mH$
p	number of pole pairs	2

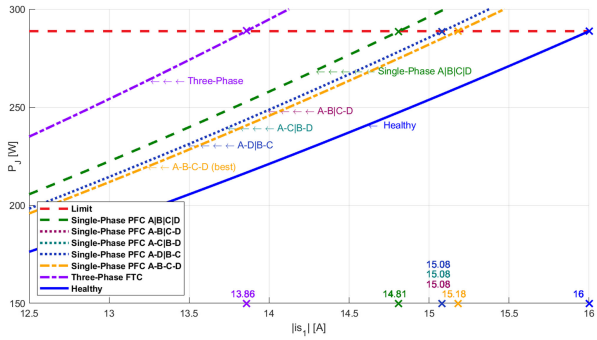

Fig. 6. Comparison of analytical stator copper losses with the healthy machine (blue) and the faulty machine (phase A1 open). "Three-phase PFC" (purple) and "single-phase PFC": quadruple-three-phase layout (green), double-six-phase layouts (spotted), and 12-phase single-star layout (yellow). The rated copper losses are highlighted in red.

open-phase fault, the control scheme of a quadruple-three-phase machine does not require any additional PI regulator if the "three-phase PFC" is implemented (purple signals in Fig. 5). Conversely, if the optimized "single-phase PFC" is used, the control system requires three additional pairs of PI regulators (green signals at the input of regulators d, e, and f). In addition, if the winding layout is a single-star type or a double-six-phase type, the number of PI regulators required to implement the "single-phase PFC" increases further. The additional regulators are necessary to control the zero-sequence currents flowing from and to different three-phase windings. In Fig. 5, the additional PIs needed in case of "single-phase PFC" are highlighted in yellow. Hence, the total number of PI regulators for the current control raises to 11 pairs.

VI. ANALYTICAL RESULTS

In this section, the postfault strategies and star connection layouts are analyzed for the quadruple-three-phase induction machine in a single-phase postfault operation.

The comparison is carried out in terms of stator copper losses and maximum phase currents by varying the magnitude of the fundamental current SV $|\bar{i}_{S,1}|$. Table I presents the main machine parameters.

Figs. 6 and 7 show the stator copper losses and the maximum phase currents, respectively, as a function of the magnitude of

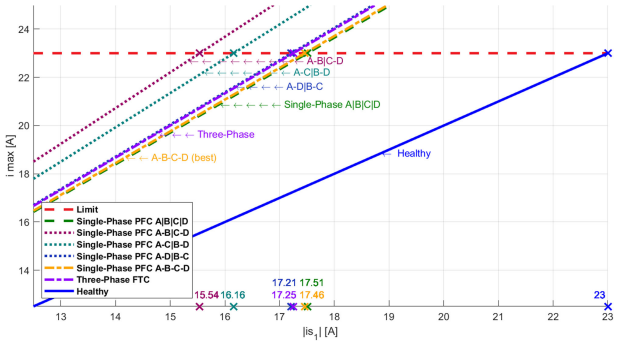

Fig. 7. Comparison of analytical maximum phase current with the healthy machine (blue) and the faulty machine (phase A1 open). "Three-phase PFC" (purple) and "single-phase PFC": quadruple-three-phase layout (green), double-six-phase layouts (spotted), and 12-phase single-star layout (yellow). The maximum phase current is highlighted in red.

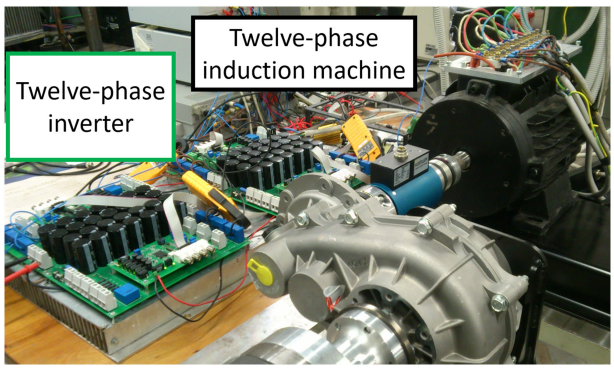

Fig. 8. Test bench: 12-phase inverter (left) and machine prototype (right).

the main current SV $|\bar{i}_{S,1}|$ and for the analyzed PFCs and star connection layouts. It is possible to notice from Fig. 6 (green line) that for a quadruple-three-phase layout $A|B|C|D$, the rated copper losses are reached at about 14.81 and 13.86 A in case of a single-phase open-fault with a "single-phase PFC" and a "three-phase PFC," respectively, compared with 16 A $|\bar{i}_{S,1}|$ in healthy conditions. Conversely, assuming a "single-star PFC," the rated losses are reached at about 15.18 A with a single-star layout, and at about 15.08 A for all the double-six-phase layouts.

Fewer differences between single-phase and three-phase PFCs have been found in terms of maximum phase currents. In fact, as illustrated in Fig. 7, the limitation on the peak current during postfault operation leads to a reduction of the maximum magnitude of $\bar{i}_{S,1}$ from 23 A, in healthy conditions, to about 17.5 A during the postfault operation. A worse result has been found for the double-six-phase layouts. The $A-B|C-D$ layout admits a maximum $|\bar{i}_{S,1}|$ value of 15.54 A, which increases to 16.16 and 17.21 A for the layouts $A-C|B-D$ and $A-D|B-C$, respectively. It is worth to note that the only result that changes with the position of the faulty phase is the peak current in the double-six-phase layout $A-D|B-C$, which in half of the cases results in the same constraint obtained for the layout $A-B|C-D$ (i.e., it admits a maximum $|\bar{i}_{S,1}|$ value of 15.54 A). Considering the worse condition in terms peak current for all the possible open-phase faults, it turns out that $A-C|B-D$ is the dual-six-phase layout and admits the highest set point for the fundamental current vector $|\bar{i}_{S,1}|$.

In the proposed control technique, the control system ensures that the magnitude of the current SV in the fundamental subspace is always kept below a threshold value, which makes the phase currents satisfy the current constraint. This threshold value depends on the fault scenario. The auxiliary current SVs are indirectly limited, being calculated from the fundamental one by (28).

In case of healthy machine, the current limitation affects the fundamental current vector (which is the only one controlled to a value that differs from zero) and is equal to the inverters' current limit.

In case of a fault, the limitation of the fundamental current SV must consider the different peak values that are reached from the remaining healthy phases. For example, for the considered machine with a rated inverter current of 23 A, the limitation of the fundamental current vector in case of a single open-phase fault corresponds to the values that are reported in Fig. 7 above the horizontal axis.

The comparisons of the stator copper losses and the peak currents show that the proposed PFC allows the continuous operation of the machine with an acceptable reduction of power. In contrast, the available overload capability is limited by a tighter constraint related to the maximum peak of the phase currents.

VII. Experimental Results

In order to experimentally assess the proposed control strategy for five different winding layouts of multiphase drive, a prototype of a quadruple-three-phase induction machine has been employed. The test bench, the quadruple-three-phase induction machine, and the multiphase inverter, commanded by a DSP TMS320F28335 controller, are shown in Fig. 8.

Fig. 9 illustrates the waveforms of the stator currents and the trajectories of the current SVs in the $\alpha\beta$ planes when the machine operates in an open-phase fault condition (the first phase of the inverter A is open). The experimental results are presented for the most significant PFC strategies (the optimum "single-phase PFC" and the simpler "three-phase PFC") and star connection layouts (quadruple-three-phase, double-six-phase, and single-star 12-phase configurations). The machine is operating at 700 r/min. The torque is 7.5 N·m and $i_{S,1,d}$ is 10 A.

The current waveforms and trajectories of the current SVs are as expected from the analytical study, except for the current ripple. The distortion of the phase currents is mainly attributed to the effects of the high-order field harmonics and the machine and converter nonlinearities. The peak values of the phase currents in the results of Fig. 9 do not show significant variations when different star connection layouts or an improved "single-phase PFC" algorithm are used. This agrees with the results presented in Fig. 7. Table II summarizes the experimental results in terms of stator copper losses and number of additional PI regulators required for effective control of the current SVs (in case of healthy and faulty machine). The results are in agreement with the expected analytical solutions with a maximum mismatch on the

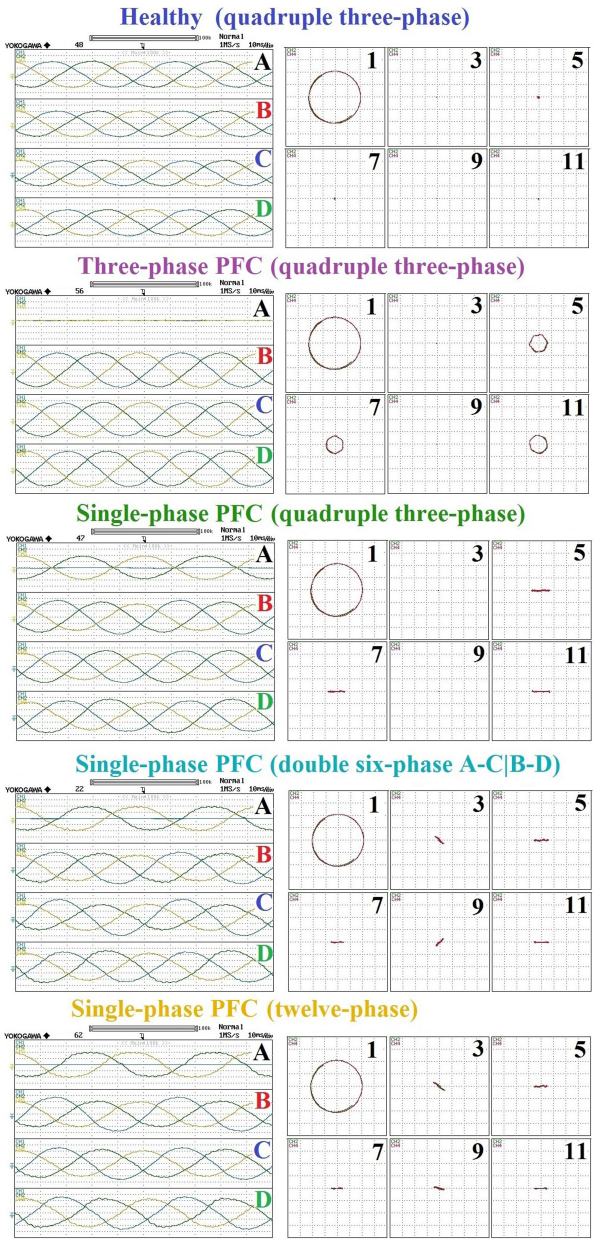

Fig. 9. Phase currents (left) and current SV trajectories (right, with in red the measured values and in green the reference values) when the machine is operating in healthy operation (first row) and in the same post fault condition (phase A1 open fault) with the most significant PFCs and star connection layouts. The scale is 5 A/div in all the subfigures.

stator copper losses of 4.6%. In terms of stator copper losses, the comparison shows significant advantages in using a single-star layout and a "single-phase PFC" over a quadruple-three-phase layout and a "three-phase PFC." However, this improvement is obtained with a more complicated control architecture. The other possible star layouts and postfault algorithms present intermediate solutions, and the selection of the layout has to be evaluated according to the considered application and its fault-tolerant requirements.

In case of a higher number of faulty phases, the advantage of using a more complicated control strategy with a reduced number of neutral points seems even more significant in terms of copper losses. However, the probability of simultaneous open-phase faults in different converters is much lower than a single-phase or a single-converter failure. Therefore, the presented analysis and the developed control strategy, together with the experimental validation summarized in Table II, can be considered as a useful guideline for the choice of the fault-tolerant design/control architecture of a multiphase drive.

TABLE II
COMPARISON OF THE PFCS (THREE-PHASE AND SINGLE-PHASE PFCS) AND STAR CONNECTION LAYOUTS FOR A SINGLE-PHASE OPEN FAULT

Post-Fault Control (Star Layout)	Copper losses W (experimental) 0.188 Ω resistance	Computational effort in N. of PIs (N. of additional PIs vs. the healthy quadruple three-phase layout)
Healthy (quadruple 3-ph)	140.3 (+ 0 %)	8
Healthy (double 6-ph)	140.9 (+ 0 %)	12 (+ 4)
Healthy (12-ph)	140.4 (+ 0 %)	12 (+ 4)
3-ph PFC (quadruple 3-ph)	181.5 (+ 29.3 %)	8 (+ 0)
3-ph PFC (double 6-ph)	181.1 (+ 28.5 %)	12 (+ 4)
3-ph PFC (12-ph)	178.5 (+ 27.1 %)	12 (+ 4)
1-ph PFC (quadruple 3-ph)	160.7 (+ 14.5 %)	14 (+ 6)
1-ph PFC (double 6-ph)	156.4 (+ 11.0 %)	16 (+ 8)
1-ph PFC (12-ph)	153.8 (+ 9.5 %)	16 (+ 8)

VIII. CONCLUSION

This article extends the PFC algorithms developed for multiphase drives under open-phase fault operation to multiphase machines with any layout of the star connections. The presented postfault strategy, based on the minimization of the stator copper losses, allows defining the optimum reference currents for symmetrical or asymmetrical multiphase windings with different star connection layouts and in any open-phase postfault operation, under the assumption of neglecting the effects of the high-order field harmonics. In fact, (28) can be directly implemented on a control platform in each fault scenario, and the optimum postfault algorithm is calculated without the need for numerical iterations. The proposed method takes into account the constraint introduced by the different star connection layouts of the n-phase subwindings, highlighting advantages and drawbacks in terms of stator copper losses, peak currents, and computational efforts (number of additional PI regulators) resulting from the winding architecture and postfault strategy. The theoretical considerations have been verified by experimental tests using a prototype of a quadruple-three-phase induction machine. This article aims to give a contribution to the state of the art in the design and control of multiphase machines for safety-critical applications.

APPENDIX

The matrices A, B, C, and F for a particular open-phase fault (phase A2) are reported in Table III. In particular, the matrices A, B, and C are used in (25)–(29) to determine the postfault matrix F. All these matrices are constant and are only related to the winding layout, the fault configuration, and the postfault strategy. Thus, they are not affected by the actual operation of the drive.

TABLE III
SUMMARY OF THE A, B, C, AND F MATRICES FOR PHASE A2 OPEN FAULT IN CASE OF SINGLE-PHASE AND THREE-PHASE PFCS AND FOR SIGNIFICANT STAR CONNECTION LAYOUTS

Matrix A (1-ph PFC)	1.000	0.000	-0.500	-0.866	-0.500	0.866	1.000	0.000	-0.500	-0.866
Matrix B (1-ph PFC)'	-0.500	0.866								
Matrix C Layout A—B—C—D' (1-ph PFC)	1.000	0.000	0.000	0.000	0.000	0.000	0.000	0.000	0.000	0.000
	0.000	1.000	0.000	0.000	0.000	0.000	0.000	0.000	0.000	0.000
	0.000	0.000	0.000	0.000	0.000	0.000	1.000	0.000	0.000	0.000
	0.000	0.000	0.000	0.000	0.000	0.000	0.000	1.000	0.000	0.000
Matrix F' Layout 'A—B—C—D'(1-ph PFC)	0.000	0.000	-0.083	-0.144	-0.083	0.144	0.000	0.000	-0.083	-0.144
	0.000	0.000	0.144	0.250	0.144	-0.250	0.000	0.000	0.144	0.250
Matrix C Layout 'A-C—B-D'(1-ph PFC)	0.500	1.000	0.000	0.000	0.000	0.000	0.500	0.000	0.000	0.000
	-0.500	0.000	0.000	0.000	0.000	0.000	-0.500	1.000	0.000	0.000
Matrix F' Layout 'A-C—B-D'(1-ph PFC)	0.063	-0.063	-0.063	-0.108	-0.063	0.108	0.063	0.063	-0.063	-0.108
	-0.108	0.108	0.108	0.188	0.108	-0.188	-0.108	-0.108	0.108	0.188
Matrix C Layout 'A-B-C-D'(1-ph PFC)	2.414	5.828	0.000	0.000	0.000	0.000	2.414	1.000	0.000	0.000
Matrix F' Layout 'A-B-C-D'(1-ph PFC)	0.083	-0.067	-0.056	-0.096	-0.056	0.096	0.083	-0.011	-0.056	-0.096
	-0.144	0.116	0.096	0.167	0.096	-0.167	-0.144	0.020	0.096	0.167
Matrix A (3-ph PFC)	1.000	0.000	1.000	0.000	1.000	0.000	1.000	0.000	1.000	0.000
	1.000	0.000	-0.500	-0.866	-0.500	0.866	1.000	0.000	-0.500	-0.866
	1.000	0.000	-0.500	0.866	-0.500	-0.866	1.000	0.000	-0.500	0.866
Matrix B (3-ph PFC)	1.000	0.000								
	-0.500	0.866								
	-0.500	-0.866								
Matrix F' (3-ph PFC)	0.000	0.000	-0.333	0.000	-0.333	0.000	0.000	0.000	-0.333	0.000
	0.000	0.000	0.000	0.333	0.000	-0.333	0.000	0.000	0.000	0.333

REFERENCES

[1] J. W. Bennett, B. C. Mecrow, D. J. Atkinson, and G. J. Atkinson, "Safety-critical design of electromechanical actuation systems in commercial aircraft," *IET Electr. Power Appl.*, vol. 5, no. 1, pp. 37–47, 2011.

[2] V. Madonna, P. Giangrande, and M. Galea, "Electrical power generation in aircraft: Review, challenges, and opportunities," *IEEE Trans. Transp. Electrific.*, vol. 4, no. 3, pp. 646–659, Sep. 2018.

[3] J. W. Bennett, G. J. Atkinson, B. C. Mecrow, and D. J. Atkinson, "Fault-tolerant design considerations and control strategies for aerospace drives," *IEEE Trans. Ind. Electron.*, vol. 59, no. 5, pp. 2049–2058, May 2012.

[4] P. Zheng, Y. Sui, J. Zhao, C. Tong, T. A. Lipo, and A. Wang, "Investigation of a novel five-phase modular permanent-magnet in-wheel motor," *IEEE Trans. Magn.*, vol. 47, no. 10, pp. 4084–4087, Oct. 2011.

[5] G. Feng, C. Lai, W. Li, J. Tjong, and N. C. Kar, "Open-phase fault modeling and optimized fault-tolerant control of dual three-phase permanent magnet synchronous machines," *IEEE Trans. Power Electron.*, vol. 34, no. 11, pp. 11116–11127, Nov. 2019.

[6] D. T. Vu, N. K. Nguyen, E. Semail, and T. J. dos Santos Moraes, "Control strategies for non-sinusoidal multiphase PMSM drives in faulty modes under constraints on copper losses and peak phase voltage," *IET Electr. Power Appl.*, vol. 13, no. 11, pp. 1743–1752, 2019.

[7] F. Yu, M. Cheng, and K. T. Chau, "Controllability and performance of a nine-phase FSPM motor under severe five open-phase fault conditions," *IEEE Trans. Energy Convers.*, vol. 31, no. 1, pp. 323–332, Mar. 2016.

[8] X. Wang, Z. Wang, Z. Xu, J. He, and W. Zhao, "Diagnosis and tolerance of common electrical faults in t-type three-level inverters fed dual three-phase PMSM drives," *IEEE Trans. Power Electron.*, vol. 35, no. 2, pp. 1753–1769, Feb. 2020.

[9] T. S. de Souza, R. R. Bastos, and B. J. Cardoso Filho, "Synchronous-frame modeling and dq current control of an unbalanced nine-phase induction motor due to open phases," *IEEE Trans. Ind. Appl.*, vol. 56, no. 2, pp. 2097–2106, Mar./Apr. 2020.

[10] X. Wang, Z. Wang, M. Gu, D. Xiao, J. He, and A. Emadi, "Diagnosis-free self-healing scheme for open-circuit faults in dual three-phase pmsm drives," *IEEE Trans. Power Electron.*, vol. 35, no. 11, pp. 12053–12071, Nov. 2020.

[11] A. Tani, M. Mengoni, L. Zarri, G. Serra, and D. Casadei, "Control of multiphase induction motors with an odd number of phases under open-circuit phase faults," *IEEE Trans. Power Electron.*, vol. 27, no. 2, pp. 565–577, Feb. 2012.

[12] H. S. Che, M. J. Duran, E. Levi, M. Jones, W. P. Hew, and N. A. Rahim, "Postfault operation of an asymmetrical six-phase induction machine with single and two isolated neutral points," *IEEE Trans. Power Electron.*, vol. 29, no. 10, pp. 5406–5416, Oct. 2014.

[13] W. N. W. A. Munim, M. J. Duran, H. S. Che, M. Bermudez, I. Gonzalez-Prieto, and N. A. Rahim, "A unified analysis of the fault tolerance capability in six-phase induction motor drives," *IEEE Trans. Power Electron.*, vol. 32, no. 10, pp. 7824–7836, Oct. 2017.

[14] F. Baneira, J. D. Gandoy, A. G. Yepes, O. Lopez, and D. P. Estevez, "Control strategy for multiphase drives with minimum losses in the full torque operation range under single open phase fault," *IEEE Trans. Power Electron.*, vol. 32, no. 8, pp. 6275–6285, Aug. 2017.

[15] A. G. Yepes, J. Doval-Gandoy, F. Baneira, and H. A. Toliyat, "Comparison of stator winding connections in multiphase drives under healthy operation and with one open converter leg," *IET Electr. Power Appl.*, vol. 14, no. 4, pp. 584–596, 2020.

[16] A. S. Abdel-Khalik, S. Ahmed, and A. M. Massoud, "Steady-state equivalent circuit of five-phase induction machines with different stator connections under open-line conditions," *IEEE Trans. Ind. Electron.*, vol. 63, no. 8, pp. 4651–4662, Aug. 2016.

[17] A. S. Abdel-Khalik, A. S. Morsy, S. Ahmed, and A. M. Massoud, "Effect of stator winding connection on performance of five-phase induction machines," *IEEE Trans. Ind. Electron.*, vol. 61, no. 1, pp. 3–19, Jan. 2014.

[18] I. Gonzalez-Prieto, M. J. Duran, H. S. Che, E. Levi, M. Bermudez, and F. Barrero, "Fault-tolerant operation of six-phase energy conversion systems with parallel machine-side converters," *IEEE Trans. Power Electron.*, vol. 31, no. 4, pp. 3068–3079, Apr. 2016.

[19] A. S. Abdel-Khalik, M. S. Hamad, A. M. Massoud, and S. Ahmed, "Post-fault operation of a nine-phase six-terminal induction machine under single open-line fault," *IEEE Trans. Ind. Electron.*, vol. 65, no. 2, pp. 1084–1096, Feb. 2018.

[20] F. Baudart, B. Dehez, E. Matagne, D. Telteu-Nedelcu, P. Alexandre, and F. Labrique, "Torque control strategy of polyphase permanent-magnet synchronous machines with minimal controller reconfiguration under open-circuit fault of one phase," *IEEE Trans. Ind. Electron.*, vol. 59, no. 6, pp. 2632–2644, Jun. 2012.

[21] G. Sala, P. Girardini, M. Mengoni, L. Zarri, A. Tani, and G. Serra, "Comparison of fault tolerant control techniques for quadruple three-phase induction machines under open-circuit fault," in *Proc. IEEE 11th Int. Symp. Diagnostics Elect. Mach., Power Electron. Drives*, Tinos, Greece, 2017, pp. 213–219.

[22] V. F. M. B. Melo, C. B. Jacobina, and N. Rocha, "Fault tolerance performance of dual-inverter-based six-phase drive system under single-, two-, and three-phase open-circuit fault operation," *IET Power Electron.*, vol. 11, no. 1, pp. 212–220, 2018.
[23] V. F. M. B. Melo, C. B. Jacobina, N. Rocha, and E. R. Braga-Filho, "Fault tolerance performance of two hybrid six-phase drive systems under single-phase open-circuit fault operation," *IEEE Trans. Ind. Appl.*, vol. 55, no. 3, pp. 2973–2983, May/Jun. 2019.
[24] A. Boglietti, I. R. Bojoi, S. Rubino, and M. Cossale, "Overload capability of multiphase machines under normal and open-phase fault conditions: A thermal analysis approach," *IEEE Trans. Ind. Appl.*, vol. 56, no. 3, pp. 2560–2569, May/Jun. 2020.
[25] N. Bianchi, E. Fornasiero, and S. Bolognani, "Thermal analysis of a five-phase motor under faulty operations," *IEEE Trans. Ind. Appl.*, vol. 49, no. 4, pp. 1531–1538, Jul./Aug. 2013.
[26] G. Sala, G. Valente, D. Gerada, P. Zanchetta, and C. Gerada, "Post-fault operation of bearingless multisector SPM machines by space vector control," *IEEE Trans. Power Electron.*, vol. 35, no. 4, pp. 4168–4177, Apr. 2020.
[27] H. Zahr, M. Trabelsi, and E. Semail, "Comparison and analysis of post-fault operation modes in a five-phase PMSM considering thermal behavior," in *Proc. IEEE 12th Int. Conf. Compat., Power Electron. Power Eng.*, 2018, pp. 1–6.
[28] Y. Zhao and T. A. Lipo, "Space vector PWM control of dual three-phase induction machine using vector space decomposition," *IEEE Trans. Ind. Appl.*, vol. 31, no. 5, pp. 1100–1109, Sep./Oct. 1995.
[29] G. Sala, M. Mengoni, G. Rizzoli, L. Zarri, and A. Tani, "Decoupled d-q axes current sharing control of multi three-phase induction machines," *IEEE Trans. Ind. Electron.*, vol. 67, no. 9, pp. 7124–7134, Sep. 2020.
[30] M. J. Duran, I. Gonzalez-Prieto, A. Gonzalez-Prieto, and F. Barrero, "Multiphase energy conversion systems connected to microgrids with unequal power-sharing capability," *IEEE Trans. Energy Convers.*, vol. 32, no. 4, pp. 1386–1395, Dec. 2017.
[31] I. Zoric, M. Jones, and E. Levi, "Arbitrary power sharing among three-phase winding sets of multiphase machines," *IEEE Trans. Ind. Electron.*, vol. 65, no. 2, pp. 1128–1139, Feb. 2018.

Giacomo Sala (Member, IEEE) received the B.Sc. degree in power engineering, the M.Sc. (hons.) degree in electrical engineering, and the Ph.D. degree in electrical machines and drives from the University of Bologna, Bologna, Italy, in 2012, 2014, and 2018, respectively.

Until 2019, he was as a Researcher with the Power Electronics, Machines and Control Group, Department of Electrical and Electronic Engineering, The University of Nottingham, Nottingham, U.K. Since 2019, he has been a Researcher with the Department of Electrical, Electronic, and Information Engineering "Guglielmo Marconi," University of Bologna, where he has been a Junior Assistant Professor, since 2020. His research interests include design, modeling, and control of multiphase electrical machines, fault-tolerant control, and fault diagnosis of electric drives.

Michele Mengoni (Member, IEEE) was born in Forlì, Italy. He received the M.S. (hons.) and Ph.D. degrees in electrical engineering from the University of Bologna, Bologna, Italy, in 2006 and 2010, respectively.

He is currently a Senior Assistant Professor with the Department of Electric, Electronic, and Information Engineering "G. Marconi," University of Bologna. His research interests include design, analysis, and control of three-phase electric machines, multiphase drives, and ac–ac matrix converters.

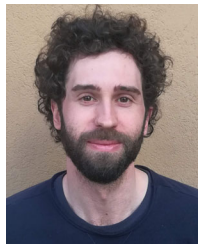

Gabriele Rizzoli received the M.Sc. (hons.) and Ph.D. (hons.) degrees in electrical engineering from the University of Bologna, Bologna, Italy, in 2012 and 2016, respectively.

He was a Visiting Student with the Center for Power Electronics, Virginia Polytechnic Institute and State University, Blacksburg, VA, USA. He is currently a Junior Assistant Professor with the Department of Electrical, Electronic and Information Engineering "G. Marconi," University of Bologna. His research interests include the design of electrical machines and the development and control of high-efficient power converters for automotive and renewable energy applications.

Dr. Rizzoli was the recipient of the Best Paper Award at the 2014 IEEE International Electric Vehicle Conference.

Michele Degano (Member, IEEE) received the master's degree in electrical engineering from the University of Trieste, Trieste, Italy, in 2011, and the Ph.D. degree in industrial engineering from the University of Padova, Padova, Italy, in 2015.

From 2014 to 2016, he was a Postdoctoral Researcher with The University of Nottingham, Nottingham, U.K., where he joined the Power Electronics, Machines and Control (PEMC) Research Group. In 2016, he joined the University of Nottingham as an Assistant Professor in Advanced Electrical Machines and became an Associate Professor in 2020. He is currently the PEMC Director of Industrial Liaison leading research projects for the development of future hybrid electric aerospace platforms and electric transports. His main research interests include electrical machines and drives for industrial, automotive, railway, and aerospace applications, ranging from small to large power.

Luca Zarri (Senior Member, IEEE) received the M.Sc. (hons.) degree in electrical engineering and the Ph.D. degree from the University of Bologna, Bologna, Italy, in 1998 and 2007, respectively.

He was a Freelance Software Programmer from 1989 to 1992, and a Plant Designer with an engineering company from 1998 to 2002. In 2003, he joined as a Laboratory Engineer with the Department of Electrical, Electronic and Information Engineering "G. Marconi," University of Bologna, where he was an Assistant Professor from 2005 to 2014, and has been an Associate Professor since 2015. He has authored or coauthored more than 100 scientific papers. His current research interests include the control of power converters and electric drives.

Dr. Zarri is a Senior Member of the IEEE Industry Applications Society, the IEEE Power Electronics Society, and the IEEE Industrial Electronics Society.

Angelo Tani was born in Faenza, Italy, in 1963. He received the M.Sc. (hons.) degree in electrical engineering from the University of Bologna, Bologna, Italy, in 1988.

He is currently a Full Professor of Power Electronics, Electrical Machines, and Drives with the Department of Electric, Electronic and Information Engineering, University of Bologna. He has authored more than 170 papers published in technical journals and conference proceedings. His current research interests include multiphase motor drives, ac–ac matrix converters, and field weakening strategies for induction motor drives.